The Journal of Prevention of Alzheimer's Disease 13 (2026) 100530

Contents lists available at ScienceDirect

The Journal of Prevention of Alzheimer's Disease

journal homepage: www.elsevier.com/locate/tjpad

Original Article

Discordance in amyloid positivity between visual reads and Centiloids: Impact of white matter uptake

Arnaud Charil *, Todd M. Nelson, Anthonin Reilhac, Viswanath Devanarayan, Shobha Dhadda, Michael C. Irizarry, Lynn D. Kramer, Larisa Reyderman

Eisai Inc., Nutley, NJ, USA

ARTICLE INFO

Keywords:
Alzheimer's disease
Amyloid positivity
Elenbecestat
Discordance
Visual reads
White matter tracer uptake

ABSTRACT

Background: The visual interpretation of amyloid PET scans, or visual read (VR), is the most common technique used in clinical practice to identify the presence of cerebral amyloid plaques. Amyloid status (positive or negative) determined by VR or using a Centiloid (CL) cut-off shows high overall concordance. However, discordant cases can occur where the VR is positive, but the CL is below the positivity cut-off, or vice versa.
Objectives: The objective of this analysis was to evaluate the rate of discordance and explore potential causes, particularly the role of amyloid tracer uptake in the white matter (WM), when determining amyloid status using VR and CL in screening for the elenbecestat phase 3 studies in early Alzheimer's disease (AD).
Design: Amyloid PET scans using either Florbetapir (Amyvid™), Florbetaben (Neuraceq™) or Flutemetamol (Vizamyl™) from 3,232 participants (1507 VR- and 1725 VR+) with cognitive impairment screened for the elenbecestat phase 3 studies in early AD were visually interpreted at screening by trained neuroradiologists and quantified using CL values.
Setting: Academic and clinical centers
Intervention/Measurements: Quantitatively, amyloid positivity was defined as CL > 32.21. The number of positive cortical regions was determined by counting the number of regions with a standardized uptake value ratio (SUVr) that exceeded 1.17. PET SUVr levels in the cerebral WM were measured using an eroded WM region of interest (ROI). Statistical tests were conducted to detect differences among the four concordance groups, defined by the relationship of VR and CL status (positive or negative). Additionally, tests examined the relationship between uptake in the WM and rates and type of discordance. Receiver operating characteristic (ROC) analysis and DeLong's test were also used to examine the effect of different tracers on the discordant rates.
Result: Discordance was observed in 6.53% of cases (n=211), with VR+/CL- in 4.61% (n=149) and VR-/CL+ in 1.92% (n=62). VR+/CL- discordant cases had significantly fewer amyloid-positive cortical regions compared to both VR+/CL+ and VR-/CL+ cases. VR-/CL+ cases had a significantly higher WM uptake than VR-/CL- and VR+/CL- cases. Our findings revealed a relationship between WM uptake and rates and types of discordance. High WM uptake can erroneously lead to CL+, due to gray matter (GM) contamination from the WM, and VR- status, due to reduced contrast between WM and GM, resulting in VR-/CL+ cases. Conversely, low WM uptake can result in an underestimation of CL values, inaccurately classifying a scan as CL-, and at the same time, the increased contrast may result in a VR+, thereby increasing the occurrence of discordant VR+/CL- cases.
Conclusion: Variations in WM uptake significantly contribute to discordances by introducing positive or negative bias in CL values and altering the GM to WM contrast, which forms the basis of the VR. Nevertheless, the rates of discordant cases are low and VR represents a robust and validated method to determine the presence of amyloid deposition. VR enables enrolling patients with amyloid beta pathology, as seen on amyloid PET scans, whereas CL scaling was developed to provide standardized units that more consistently characterize longitudinal amyloid-β change. These findings reflect the complementary roles of VR and CL in amyloid PET evaluation, with implications for refining diagnostic accuracy and disease monitoring in AD clinical trials and practice.

* Corresponding author: 200 Metro Blvd, Nutley, NJ 07110, USA.
E-mail address: arnaud_charil@eisai.com (A. Charil).

https://doi.org/10.1016/j.tjpad.2026.100530
Received 20 December 2025; Received in revised form 30 January 2026; Accepted 16 February 2026
Available online 14 March 2026

Introduction

The defining central nervous system (CNS) pathology in Alzheimer's disease (AD) is characterized by the presence of amyloid plaques, which are extracellular deposits of amyloid beta (Aβ) protein, and neurofibrillary tangles (NFT) [1]. Positron emission tomography (PET) radiotracers enabling amyloid to be imaged in vivo allows determining the presence of amyloid in the living patient. Three PET ligands for Aβ are currently approved for clinical use by the European Medicines Agency, the US Food and Drug Administration, and other regulatory agencies around the world: Florbetapir (Amyvid™), Florbetaben (Neuraceq™) and Flutemetamol (Vizamyl™) [2]. The visual interpretation of an amyloid PET scan – the so-called visual read (VR) – is performed according to each manufacturer's guidelines, and although slight differences exist in the way the scans are read, the three approved VR protocols show good agreement in classifying a scan as amyloid positive or negative [3]. VRs are the most common method to determine the presence of cerebral amyloid pathology in clinical practice.

In addition to the VR, the amount of amyloid can be quantified using various imaging processing pipelines that generate the standardized uptake value ratio (SUVr). To account for variations in the SUVr range and properties between tracers, these values can be standardized using the Centiloid (CL) scale, as outlined in the published guidelines [4–5]. Once converted to the CL scale, each individual amyloid PET scan can be quantitatively classified as either CL positive or negative based on whether the CL value exceeds or falls below a prespecified threshold for positivity. When this threshold is determined in such a way that it optimally separates VR positive and negative PET scans, for instance through ROC analysis, amyloid status (positive or negative) determined by either a qualitative VR or a quantitative CL cut-off shows good overall concordance. However, it is not uncommon to encounter discordant cases, where the VR is positive, but the CL is below a positivity cut-off, or vice versa [6–7]. While the existence of discordant cases is not surprising due to the fundamentally different classification methods, it is important to understand and consider the differences between amyloid positivity determined by either VR or a CL cut-off.

The objectives of this analysis were to assess the rates of amyloid status discordance between VR and CL methods and explore possible reasons for these discordances in the screening for two elenbecestat phase 3 studies. Elenbecestat is a BACE inhibitor, where BACE (β-site amyloid precursor protein cleaving enzyme) is an enzyme involved in the production of β-amyloid. This program included two global phase 3 studies (NCT02956486; NCT03036280) in subjects with early AD (i.e., mild cognitive impairment [MCI] due to AD or mild AD dementia with amyloid positivity confirmed by PET VR or CSF) [8]. Of particular interest in explaining amyloid status discordance was the hypothesis that intersubject variability in tracer uptake within the WM influences both the VR and CL values of amyloid PET scans, a concept that has not been previously explored.

Methods

Patients

A total of 9758 subjects were screened across 29 countries. Subjects advanced to amyloid PET imaging if they met the National Institute of Aging – Alzheimer's Association (NIA-AA) core clinical criteria for AD or MCI, had an Mini-Mental State Examination (MMSE) score ≥24, a Clinical Dementia Rating (CDR) of 0.5, were between 50 and 85 years of age, and satisfied all inclusion and exclusion requirements. Only participants who were amyloid-positive by either VR PET scan or CSF assessment were eligible for randomization (n=2212) and subsequently received either placebo or 50 mg QID Elenbecestat [8]. Approval was obtained from the Institutional Review Board or independent ethics committee at each center, with all participants providing written informed consent. Of the total 9758 screened subjects, 3232 early AD subjects were considered for evaluation in this current study (1507 were VR- and 1725 were VR+).

Image acquisition and processing

Contingent on accessibility to the tracer manufacturing facilities, either one of the three approved amyloid PET tracers was used in the sample we analyzed (i.e., Florbetapir (Amyvid™) = 8.3 %, Florbetaben (Neuraceq™) = 74.8 % or Flutemetamol (Vizamyl™) = 16.9 %). Patients underwent a 20-minute PET scan 90 ± 1 min after receiving an injection of Florbetaben (300 MBq) or Flutemetamol (185 MBq), or 50 ± 1 min following an injection of Florbetapir (370 MBq).

The following steps are part of a standardized image-processing pipeline implemented by BioClinica. First, all 4 × 5 min amyloid PET frames were rigidly co-registered to the first frame, motion-corrected, averaged into a static image, smoothed to harmonize resolution across sites, and co-registered to the patient's 3D T1-weighted magnetic resonance imaging (MRI). Using each subject's 3D T1-weighted MRI, 74 brain regions were segmented using the Desikan-Killiany atlas [9]. and mapped onto the amyloid PET data to extract regional SUVr values. Additionally, a composite cortical amyloid PET SUVr was computed as the average of the frontal, temporal, parietal, and cingulate cortices, using the whole cerebellum as the reference region. The mean composite SUVr, obtained using either amyloid tracer, was converted into CLs, a 100-point scale which has an average value of zero in "high certainty" amyloid negative subjects and an average of 100 in "typical" AD patients [4–5]. Specific SUVr to CL conversion equations have been published previously [8].

Visual reads

For the eligibility review, one of three trained neuroradiologist readers performed a single reading at baseline, and if needed, they consulted each other to reach consensus agreement on images difficult to interpret. These readers, blinded to cognitive status, centrally determined amyloid PET positivity or negativity by VR according to each tracer's manufacturer guidelines. The VR classification of the amyloid status is based on the grey matter (GM) uptake being equal to or higher than the uptake in the WM in at least one region, as per the manufacturer's guidelines for each tracer [10]. Brain regions assessed and positive scan criteria are summarized in Supplementary **Table S1**. Although scanning protocols are relatively similar across tracers, U.S. Food and Drug Administration- and the European Medicines Agency-approved VR protocols differ among the three tracers. However, Bischof et al. [3]. showed comparability of the three approved VR protocols to classify a scan as amyloid positive or negative with high interrater agreement despite applying different VR protocols for all three ^{18}F-labeled amyloid tracers.

Determination of quantitative thresholds and scan classification

A CL threshold of 32.21 – which corresponds to ~1.17 SUVr for all tracers – was determined, based on the screening data from these two phase 3 studies of Elenbecestat, to separate amyloid-positive from amyloid-negative PET scans. This threshold was determined by maximizing the Youden index (sensitivity + specificity – 1) in a ROC analysis, using VR classification as the reference standard, and it aligns with previously published thresholds [11].

Additionally, we defined an individual cortical region as being amyloid positive when SUVr > 1.17 and computed the total number of amyloid-positive cortical regions from the Desikan-Killiany atlas [9]. in each individual subject. Amyloid PET scans were classified into four groups based on the amyloid status given by the VR and the CL classification: VR-/CL-, VR+/CL-, VR-/CL+ and VR+/CL+.

Data analysis

The rate of discordant cases was determined for the full data set and separately for each amyloid PET tracer, expressed as a percentage of the total number of cases. To evaluate the relationship between VR status and CL values, ROC curves were generated for each tracer. Differences between ROC curves across tracer subgroups were assessed using DeLong's test. Fisher's exact test was used to compare discordance rates between each pair of the three amyloid PET tracers, as well as between the two discordant subgroups.

To compare continuous variables (age, MMSE, CDR sum of boxes, and the number of amyloid-positive cortical gray matter regions) across concordance groups, the Kruskal–Wallis test was used, followed by Dunn's post hoc test with Bonferroni correction. Categorical variables (baseline diagnosis, gender, and tracer type) were analyzed using chi-square tests. The use of nonparametric tests was driven by the skewed distributions observed in the concordant groups: VR+/CL+ cases were skewed toward higher positive region counts, while VR-/CL- cases showed lower counts, as described in the Results section.

Amyloid PET SUVr levels measured in cerebral WM, measured using an eroded WM ROI to minimize GM contamination, were compared across concordance groups using the Kruskal-Wallis test followed by Dunn's post hoc test with Bonferroni correction.

To further investigate WM uptake patterns, linear regression analyses were conducted to examine associations between WM SUVr and age, gender, and tracer type.

All statistical analyses were performed using JMP (version 17.2) and R (version 4.3.2). Graphs were generated in R using the ggplot2 package (version 3.5.1). Dunn's post hoc tests and ROC analyses, including DeLong's test, were conducted in R using the PMCMRplus (v.1.9.10; [12]) and pROC (v.1.18.5; [13]) packages, respectively. All other statistical tests were performed in JMP.

Results

This analysis included data from 3232 participants aged 50–85, including both eligible individuals and screening failures. Participants were clinically diagnosed with either MCI due to AD (87.7 %) or mild AD dementia (12.3 %) and not confirmed until PET scan and/or VRs of amyloid PET scans – using Florbetaben, Florbetapir, or Flutemetamol – were performed at screening by trained neuroradiologists. Participant demographics by VR/CL concordance status are summarized in Table 1.

Table 1
Demographics by visual read/Centiloid concordance status.

	VR-/CL- n=1445	VR+/CL- n=149	VR-/CL+ n=62	VR+/CL+ n=1576
Amyloid PET Centiloids, mean (SD)	-0.5 (10.8)	13.1 (15.3)	48.4 (13.7)	90.4 (30.5)
Baseline Diagnosis, n (%)				
MCI due to AD	1327 (92)	130 (87)	57 (92)	1319 (84)
Mild AD	118 (8.2)	19 (13)	5 (8.1)	257 (16)
PET Tracer, n (%)				
Florbetaben	1160 (80)	120 (81)	34 (55)	1103 (70)
Florbetapir	86 (6.0)	12 (8.1)	8 (13)	162 (10)
Flutemetamol	199 (14)	17 (11)	20 (32)	311 (20)
Gender, n (%)				
Female	745 (52)	61 (41)	42 (68)	829 (53)
Male	700 (48)	88 (59)	20 (32)	747 (47)
Age, mean years (SD)	68.6 (8.3)	71.1 (7.5)	72.9 (6.8)	72.2 (7.1)
CDR-SB, mean (SD)	2.2 (1.0)	2.5 (1.0)	2.3 (0.9)	2.4 (1.0)
MMSE, mean (SD)	26.8 (1.7)	26.7 (1.8)	26.7 (1.8)	26.4 (1.8)

AD, Alzheimer's Disease; CDR-SB, Clinical Dementia Rating Scale Sum of Boxes; MCI, Mild Cognitive Impairment; MMSE, Mini-Mental State Examination; SD, Standard Deviation; VR, Visual Read; CL, Centiloid.

A significantly higher proportion of males was observed in the VR+/CL- group (59 % vs 41 % females) compared to other groups (all p-values < 0.05). Conversely, the VR-/CL+ group had a significantly higher proportion of females (68 % vs 32 % males; all p-values < 0.05).

The overall concordance rate was 93.47 %, with VR+/CL- discordance at 4.61 % and VR-/CL+ discordance at 1.92 % (**Table S2**). Discordance rates revealed that Flutemetamol had the highest proportion of VR-/CL+ cases, while Florbetaben had the highest proportion of VR+/CL- cases. Fisher's exact test indicated significant differences in VR-/CL+ discordance between Florbetaben and the other two tracers, and a significant difference in VR+/CL- discordance only between Florbetaben and Flutemetamol (**Table S3**).

ROC analysis showed excellent agreement between VR and CL-based amyloid status for all tracers, with AUC values > 0.95 (**Table S4**). DeLong's test showed a statistically significant, though modest, difference between the ROC curve for Flutemetamol and those of the other two tracers (**Table S5**). Sensitivity, specificity, and balanced accuracy were all above 0.9 across tracers, indicating strong overall concordance (**Table S6**).

The effect of site/scanner on the relationships between the primary variables of interest (i.e., number of positive cortical GM regions, CL, WM SUVr, and concordance status) was negligible; therefore, this covariate was not included in the analyses.

Fig. 1 illustrates the number of positive cortical GM regions vs CL, with the CL threshold for positivity of 32.21 indicated by the red vertical line. The graph shows that a minimum of 30 to 40 positive regions out of 74 is required for a scan to exceed the CL threshold. Notably, some scans are VR+ despite having fewer than 10 amyloid-positive regions, resulting in a CL value well below the threshold (see Fig. 1, VR+/CL- scans represented by blue dots). Conversely, a few scans have more than 30 amyloid-positive regions while being VR- (see Fig. 1, the VR-/CL+ scans represented by pink dots).

Representative amyloid PET scans from each VR/CL group are displayed in Fig. 2. VR-/CL- scans showed no cortical region uptake above the WM levels. In contrast, VR+/CL+ cases exhibit large cortical regions with uptakes equal to or higher than in the cerebral WM. Among the VR+/CL- discordant cases, two distinct patterns were observed: [1]. "borderline" scans with minimal cortical uptake and questionable positivity (e.g., Florbetaben case), and [2]. clearly positive-appearing scans with diffuse GM uptake but unexpectedly low CL values (e.g., Florbetaben case with CL = 15). It is important to note that in the two presented VR+/CL- scans, the tracer uptake in the WM appears weaker than in the concordant cases. Finally, most VR-/CL+ discordant cases exhibited a fully negative scan pattern, as illustrated by the Florbetapir example in Fig. 2. However, a few "borderline" cases could have been classified as VR+/CL+ due to debatable loss of GM/WM contrast in limited areas (see the Florbetaben example). Additionally, unlike the VR+/CL- cases, the two VR-/CL+ examples showed stronger WM uptake than 'normal' cases (i.e., the concordant cases).

Figure S1 shows that WM SUVr was similar between the concordant groups (VR−/CL− and VR+/CL+) but differed significantly in discordant groups. The VR+/CL− group exhibited lower WM SUVr, while the VR−/CL+ group showed higher WM SUVr. These findings support the visual impressions from Fig. 2. Within each group, CL values were color-coded, showing a positive association between CL and WM SUVr.

Figure S2 shows the same analysis stratified by tracer, showing that WM uptake differences between groups exist with varying magnitudes across the three amyloid tracers.

Fig. 3 displays the number of amyloid-positive regions by VR/CL group, with points colored by WM SUVr. The VR+/CL- group had a similar range of positive regions as the VR-/CL- group (0–43 *vs* 0–45, but lower WM uptake. Notably, scans with fewer than 10 positive regions generally had very low WM uptake. Similarly, VR-/CL+ scans show comparable number of positive regions to the VR+/CL+ scans (30–76 *vs*

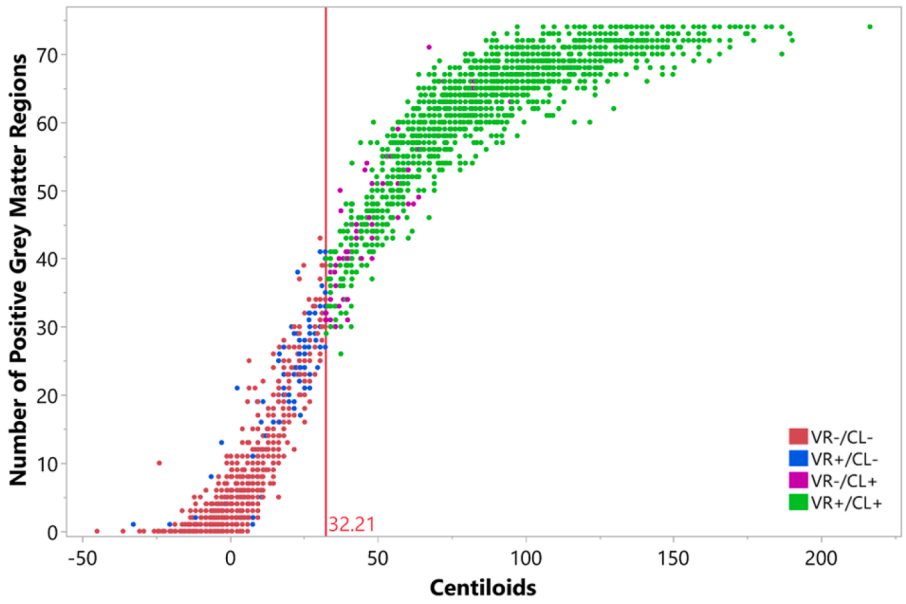

Fig. 1. Number of positive cortical gray matter regions (defined using a cut-off of SUVr = 1.17) vs Centiloids by VR/CL group (red: VR-/CL-, blue: VR+/CL-, pink: VR-/CL+, green: VR+/CL+). VR, Visual Read; CL, Centiloid.

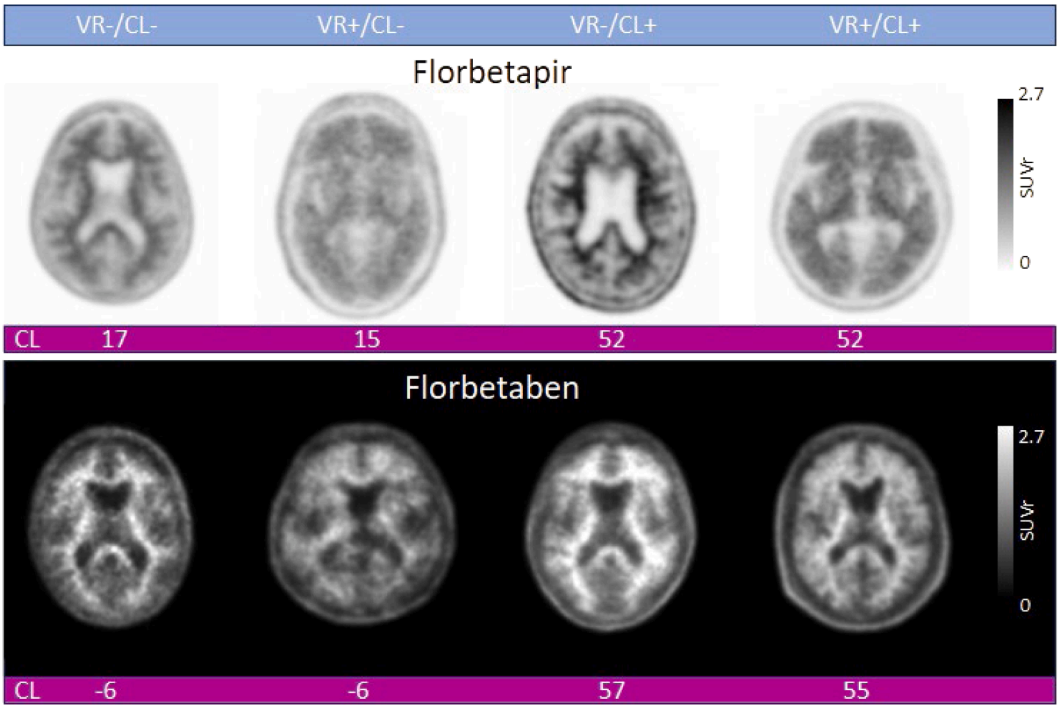

Fig. 2. Representative examples of amyloid PET scans (top row: Florbetapir, bottom row: Florbetaben) from each group (VR-/CL-, VR+/CL-, VR-/CL+, VR+/CL+). VR, Visual Read; CL, Centiloid.
The palettes shown reflect the label-recommended display settings routinely used for clinical visual interpretation. Flutemetamol images are not included because the manufacturer-recommended color palette resulted in examples that were less visually informative for illustrating the features highlighted in this figure.

28–79), but with higher WM uptake. These patterns further support the positive association between WM uptake and the number of positive regions, and consequently CL values, as seen in **Figure S1**.

Fig. 4 shows the relative proportion of scans within each VR/CL group for increasing WM uptakes. This graph clearly illustrates the relationship between WM uptake and the rates and types of discordant cases. Notably, the number of VR+/CL- cases (in blue) increases with lower WM uptake, while higher WM uptake is associated with a greater proportion of VR-/CL+ cases (in pink).

Finally, linear regression analysis showed that WM amyloid PET SUVr was significantly associated with age, gender, and amyloid tracer type (all p-values < 0.001; **Table S7**).

Discussion

Visual assessment of amyloid PET scans by trained radiologists is a common qualitative method to determine the presence of amyloid deposition in the brain and categorize a subject as being amyloid-

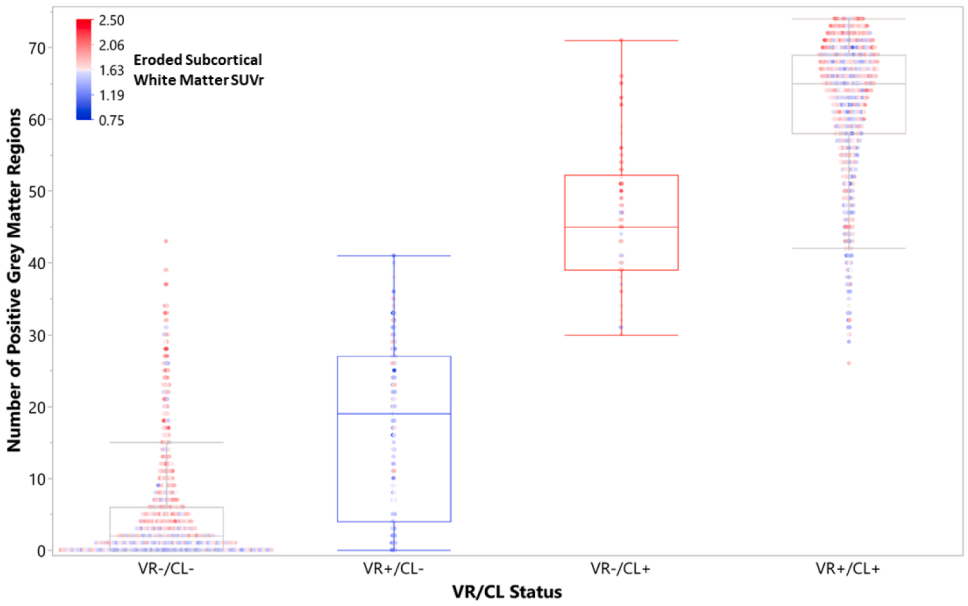

Fig. 3. Boxplots showing VR/CL group differences in the number of positive regions.
Dot color represents white matter uptake, ranging from blue (below the sample mean SUVr) to red (above the sample mean SUVr). The mean numbers of positive regions by VR/CL group are all statistically significant at p-values < 0.0001 using the Kruskal-Wallis and Dunn Tests with Bonferroni correction. WM, white matter. VR, Visual Read; CL, Centiloid.

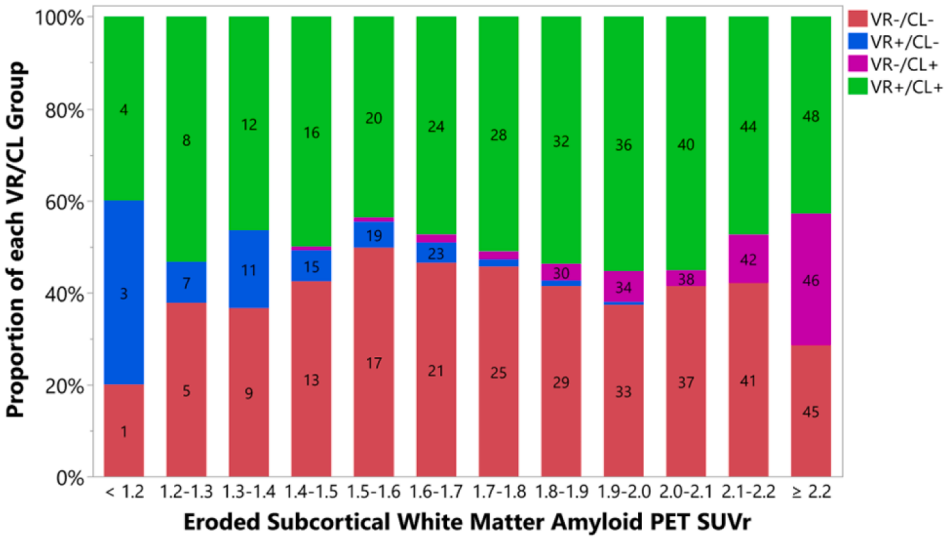

Fig. 4. Proportion of each concordance group as a function of *white matter* amyloid PET SUVr. VR, Visual Read; CL, Centiloid.

positive or -negative, which is critical for determining eligibility in anti-amyloid clinical trials [6–7]. Another approach to determine the presence of amyloid in the cortex is to quantitatively measure amyloid levels in the brain by processing PET images with a computerized algorithm to produce SUVr values for various cortical and non-cortical regions, or for the whole cortex [14]. Global SUVr values can then be converted into CL values for comparability between the different amyloid tracers [4–5]. Finally, amyloid status is then classified using a CL threshold, defined either *a priori* or, as in this study, empirically based on ROC analysis. The degree of agreement between VR-based and CL-based classifications remains a central issue in both research and clinical trial screening.

Using data from 3232 participants screened for the phase 3 studies of elenbecestat in early AD, we observed a high agreement between VR and CL classifications, with an overall concordance rate of 93.5 %. Discordances were 4.61 % for VR+/CL- and 1.92 % for VR-/CL+. These results are in line with a multicenter study where binary VR of Flutemetamol showed a very high agreement (93 % - 99 %) with quantitative amyloid level measures obtained using a variety of software tools [15]. Thurfjell et al. [16]. and Matsuda et al. [17]. also reported a high concordance rate between quantitative PET measures (Flutemetamol) and VR, ranging from 97.1 % to 99.4 % depending on the selection of reference and composite regions, and 94.6 %, respectively. Mountz et al. [18]. reported a VR/SUVr (Flutemetamol) classification agreement of 82.6 %, whereas our study showed a higher agreement of 93.23 % for the same tracer. In Zeltzer et al. [7], the concordance between VR and quantitative measures of Florbetaben, Florbetapir and Flutemetamol PET scans was 86.3 % using an *a priori* defined threshold of 24.4 CL. The rates of VR+/CL- and VR-/CL+ were 8 % and 6 %, respectively, which are higher than the rates reported in our study.

Our results suggest that discordance is not confined to cases near the CL threshold, nor is it solely attributable to threshold choice, quantification variability or borderline scans. As shown in Fig. 1, VR+/CL- cases

can have very low CL values, and VR-/CL+ cases can have very high CL values. These findings are consistent with previously studies [6–7].

The presence of discordant cases is not surprising given the inherent differences between VR and quantitative classification methods. Quantitative measures, such as amyloid PET SUVr and CL values, are derived from the quantification of the tracer uptake in a predefined ROIs relative to the tracer uptake measured in a reference region, such as the whole cerebellum, using computerized algorithms to process PET images. In contrast, VR relies on the subjective interpretation by trained radiologists, who assess GM regions for tracer uptake equal to or higher than that present in the WM. These methodological differences can naturally lead to discrepancies in classification outcomes, resulting in discordant cases. For example, a scan may be classified as positive based on the visual identification of a few focal areas of tracer uptake, even if other cortical regions appear negative (see Fig. 2, Florbetaben VR+/CL- case). When these scans are quantitatively processed to generate a global amyloid level, the positive amyloid signal, if confined to only a few regions, gets averaged over a relatively large volume. This dilution effect can lower the overall CL value and result in a CL- classification despite a positive VR.

Several approaches have been proposed to mitigate the underestimation of focal uptake by global metrics Fakhry-Darian et al [19]. suggested using region-specific SUVr thresholds, while Nai et al [20]. showed that taking the highest SUVr value, among all measured regions in the brain, rather than mean global SUVr, yielded higher agreement between VR and SUVr. This approach is intuitively closer to the visual assessment process, considering focal uptake. Conversely, diffuse cortical uptake that does not exceed adjacent WM may yield CL+, but VR- classifications (i.e., VR-/CL+ discordant cases, Fig. 2).

Influence of WM uptake on the occurrence of discordant cases

In addition to the above reasons that are commonly cited in similar studies, our results underscore the substantial variability in amyloid tracer uptake within the WM, with SUVr values ranging from 0.85 to 2.3 (**Figure S1**). More importantly, our findings reveal an important relationship between WM signal and both the rates and type of discordant cases (Fig. 4). Our interpretation is that high WM uptake increases the likelihood of VR-/CL+ cases. First, due to inflated CL in VR- scans, which is caused by direct contamination of the measured cortical GM SUVr by tracer signal coming from adjacent WM; and second, due to CL+ scans being misclassified as VR-, because of reduced GM/WM contrast. Conversely, low WM uptake favors the emergence of VR+/CL- cases due to an underestimated CL in VR+ scans - caused by lower contamination from the WM, and due to the CL- scans being incorrectly labeled as VR+ because of increased GM/WM contrast. Consequently, variations in WM uptake can influence both VR and CL. The VR+/CL- discordant group is partly composed of VR+/CL+ scans that have lost their CL positivity, and VR-/CL- scans that have gained VR positivity due to low WM uptake (**Figure S1**). Conversely, the VR-/CL+ group emerges at high WM uptake levels and is partly composed of VR-/CL- gaining CL positivity, and VR+/CL+ losing their VR positivity.

Alterations in CL values due to low or high WM uptake are closely related to the partial volume effect in PET imaging [21], whereby the signal measured in relatively small or thin regions, such as the cortical GM, is contaminated by signal originating from neighboring regions such as the WM. The magnitude of this contamination depends on several factors, including image spatial resolution, voxel size, thickness of the cortical ribbon, and the definition of the target ROI. Typically, about 20 % to 50 % of the WM signal can be measured within the target GM ROI. Consequently, any deviation in WM uptake from the "norm" (e.g., the mean WM uptake across the cohort) results in inaccuracies in CL, whereby for a given true GM uptake, high WM uptake results in overestimated CL values, while low WM uptake results in underestimated CL values.

This contamination of CL by the WM uptake is visible in **Figure S1** and Fig. 3, where within each group, there is a noticeable positive relationship between WM uptake and CL values. This contamination is however more perceptible in **Figure S3** showing the scatter plot of WM amyloid tracer uptake vs the cortical GM SUVr. If we focus on the scans with low amyloid uptake (i.e., VR-/CL- group, red dots), we can see a positive association between WM uptake and cortical SUVr values – and consequently, CL values – as illustrated by the solid red line. For instance, when the WM SUVr is above 1.9, there is no scan showing composite cortical GM SUVr under 0.9, while these scans are common when the WM SUVr is below 1.5. We can assume that the relationship between WM uptake and GM SUVr remains consistent for scans with higher GM SUVr values – illustrated by the red dashed line – especially around the SUVr threshold, represented by the black vertical dashed line, which shows the separation between negative and positive scans based on their SUVr value only, while the tilted red dashed line separates negative and positive scans based on their SUVr value while accounting for the contamination coming from the WM. Therefore, VR+/CL- scans (e.g., blue dots and arrows) in the lower triangle formed by the two intersecting red and black dash lines are CL+ scans that have lost CL positivity due to low WM uptake. In contrast, the VR-/CL+ scans (e.g., pink dots and arrows) in the upper triangle, formed by the two intersecting red and black dashed lines, are CL- that gained positivity due to high WM uptake.

If we assume a 30 % contamination on average for this cohort and using the SUVr to CL equations for the three tracers [8], any WM uptake variation of 0.1 SUVr from the mean results in a variation of 3.6 CL for Florbetaben, 4.2 CL for Florbetapir and 3 CL for Flutemetamol. Using these values, we find that 20 % VR+/CL- cases (n=30) of our cohort are VR+/CL+ cases that lost CL positivity due to low WM uptake and 32 % of the VR-/CL+ discordant scans (n=21) are VR-/CL- scans that are CL+ due to a high WM uptake. At the same time, 0.5 % of the VR-/CL- (n=7) are actually CL+ and 0.5 % of the VR+/CL+ scans (n=8) are CL-. **Figure S4** shows the impact of accounting for a 30 % WM contamination on the CL values and status. Actual cases with CL status changes are given in supplementary **Figure S5**.

Factors influencing the variability of tracer uptake in white matter

While studies on the characterization of amyloid tracers in the WM, mainly using [^{11}C]PiB PET, has shown that the binding to WM is mainly non-saturable and non-specific [22–23], the precise nature and underlying mechanism of this binding remain poorly understood. Our analysis revealed strong associations between WM uptake and factors such as age, gender, and the type of amyloid tracer used. The strong positive association with age is in line with previous studies showing very similar coefficients [24–25]. The association with gender partially accounts for the higher proportion of males in the VR+/CL- group and females in the VR-/CL+ group, a pattern that has been observed previously without identifying the main reasons [7]. Indeed, the lower binding of the amyloid tracer to the WM observed in males results in a higher proportion of males in the VR+/CL- group (59 %) while the higher binding in females accounts for the greater proportion of females in the VR-/CL+ group (68 %) (Table 1). Further studies are warranted to elucidate the basis of these sex differences in WM tracer binding, which may involve sex specific brain structural features and/or hormonal influences, or be related to cerebrovascular disease such as WM hyperintensities [26–28]. and cerebral microbleeds [25]. However, these associations were not studied here but merit future investigation.

Other potential causes of discordance

Image quality and processing pipeline may contribute to discordant cases. Subject motion can degrade image quality, affect VR due to reduced GM/WM contrast, and distort CL values. Inaccurate CL values may also result from misregistration of target or reference ROIs. While not observed in this study, truncation of the cerebellum, a common

reference region, on scanners with limited axial field-of-view can lead to inflated cortical CL values.

In this study, both VR and quantitative analyses were performed on motion-corrected, spatially harmonized images. However, in other studies, VR is often performed on minimally processed images, introducing another potential source of discordance.

Finally, threshold selection plays a role. Higher thresholds can result in VR+/CL- cases, while a lower threshold can lead to VR-/CL+ cases. In this study, the 32.21 CL threshold was empirically derived to maximize VR- vs. VR+ separation. However, several *a priori* CL thresholds have been reported in the literature for classifying amyloid PET scans [29, 30], including 24.4 CL, which represents a pathologically validated cutoff corresponding to intermediate-to-high amyloid burden [31]. As shown in **Table S8**, moving substantially away from the empirically derived threshold increases discordance rates. Nonetheless, our findings remain robust across reasonable threshold variations as the ROC analysis demonstrated that moderate changes in the CL threshold did not materially affect our conclusions.

In summary, VR is a robust and validated method to determine the presence of amyloid deposition in the brain. When performed according to the FDA-approved labeling for amyloid PET tracers, VR can support the clinical diagnosis of AD, inform disease management decisions, and confirm eligibility for anti-amyloid therapies. Conversely, CLs are better suited for assessing longitudinal changes over time by providing a quantitative and more sensitive measure to assess disease progression [4,14]. Variations in WM uptake significantly contribute to discordances by introducing positive or negative biases in CL values and altering the GM to WM contrast, which is fundamental to the VR. Together, these findings highlight the complementary strengths of VR and CL approaches, while underscoring the need to account for WM signal variability to ensure accurate and consistent interpretation of amyloid PET scans in both clinical and research settings.

Declaration of generative AI and ai-assisted technologies in the writing process

No generative AI and AI-assisted technologies were used in the writing process of this work nor to create the figures, images and artwork.

Data availability

The data are available from the corresponding author upon reasonable request.

Funding

Writing support was funded by Eisai Inc. and Biogen, in compliance with Good Publication Practice 4 ethical guidelines.

CRediT authorship contribution statement

Arnaud Charil: Writing – review & editing, Writing – original draft, Visualization, Methodology, Investigation, Formal analysis, Conceptualization. **Todd M. Nelson:** Writing – review & editing, Writing – original draft, Methodology, Investigation, Formal analysis, Conceptualization. **Anthonin Reilhac:** Writing – review & editing, Writing – original draft, Investigation, Formal analysis, Conceptualization. **Viswanath Devanarayan:** Writing – review & editing, Writing – original draft, Methodology, Formal analysis, Data curation, Conceptualization. **Shobha Dhadda:** Writing – review & editing, Writing – original draft, Methodology, Investigation, Formal analysis, Conceptualization. **Michael C. Irizarry:** Writing – review & editing, Writing – original draft, Methodology. **Lynn D. Kramer:** Writing – review & editing, Supervision, Investigation, Funding acquisition, Conceptualization. **Larisa Reyderman:** Writing – review & editing, Writing – original draft, Supervision, Methodology, Funding acquisition, Formal analysis, Data curation, Conceptualization.

Declaration of competing interest

The authors declare the following financial interests/personal relationships which may be considered as potential competing interests:

Arnaud Charil reports a relationship with Eisai that includes: employment.

Todd M. Nelson reports a relationship with Eisai that includes: employment.

Anthonin Reilhac reports a relationship with Eisai that includes: employment

Viswanath Devanarayan reports a relationship with Eisai that includes: employment

Shobha Dhadda reports a relationship with Eisai that includes: employment

Michael Irizarry reports a relationship with Eisai that includes: employment

Lynn Kramer reports a relationship with Eisai that includes: employment

Larisay Reyderman reports a relationship with Eisai that includes: employment.

Acknowledgements

We thank the patients, their families, and the sites for participating. The authors acknowledge editorial support of J. D. Cox, PhD (Mayville Medical Communications) and Lisa Yarenis (Eisai Inc.). Editorial support, funded by Eisai Inc, was provided by Mayville Medical Communications.

The authors did not receive remuneration for their participation in the preparation, review and approval of this manuscript. The sponsor, Eisai Inc., designed the research and analyzed the data, provided trial drug, provided funding for medical writing, and drafted the manuscript.

Funded by Eisai Inc and Biogen; ClinicalTrials.gov numbers: NCT02956486; NCT03036280

Supplementary materials

Supplementary material associated with this article can be found, in the online version, at doi:10.1016/j.tjpad.2026.100530.

References

[1] Scheltens P, Blennow K, Breteler MMB, de Strooper B, Frisoni GB, Salloway S, et al. Alzheimer's disease. Lancet 2016;388:505–17.
[2] Chapleau M, Iaccarino L, Soleimani-Meigooni D, Rabinovici GD. The role of amyloid PET in imaging neurodegenerative disorders: a review. J Nucl Med 2022; 63:13S–9S.
[3] Bischof GN, Bartenstein P, Barthel H, van Berckel B, Doré V, van Eimeren T, et al. Toward a universal readout for 18 F-labeled amyloid tracers: the CAPTAINs Study. J Nucl Med 2021;62:999–1005.
[4] Klunk WE, Koeppe RA, Price JC, Benzinger TL, Devous MD, Jagust WJ, et al. The Centiloid Project: standardizing quantitative amyloid plaque estimation by PET. Alzheimer's. Dementia 2015;11:1–15. .e4.
[5] Centiloid Project. 2025. Available at: http://www.gaain.org/centiloid-project. Accessed 31 October 2025.
[6] Collij LE, Bischof GN, Altomare D, Bader I, Battle M, García DV, et al. Quantification supports Amyloid PET visual assessment of challenging cases: results from the AMYPAD diagnostic and Patient Management study. J Nucl Med 2024;124:268119.
[7] Zeltzer E, Schonhaut DR, Mundada NS, Blazhenets G, Perez JM, Soleimani-Meigooni D, et al. Concordance between amyloid-PET quantification and real-world visual reads: results from IDEAS. medRxiv 2024 2024. 10.31.24316518.
[8] Roberts C, Kaplow J, Giroux M, Krause S, Kanekiyo M. Amyloid and APOE status of screened subjects in the Elenbecestat MissionAD Phase 3 program. J Prev Alzheimer 19s Dis 2021;8:218–23.
[9] Desikan RS, Ségonne F, Fischl B, Quinn BT, Dickerson BC, Blacker D, et al. An automated labeling system for subdividing the human cerebral cortex on MRI scans into gyral based regions of interest. Neuroimage 2006;31:968–80.

[10] Rabinovici GD, Knopman DS, Arbizu J, Benzinger TLS, Donohoe K, Hansson O, et al. Updated appropriate use criteria for amyloid and tau PET. Alzheimer's Dement 2023;19.
[11] Fleisher AS, Chen K, Liu X, et al. Using positron emission tomography and Florbetapir F 18 to image cortical amyloid in patients with mild cognitive impairment or dementia due to Alzheimer disease. Arch Neurol 2011:1404–11.
[12] Robin X, Turck N, Hainard A, Tiberti N, Lisacek F, Sanchez JC, Müller M. pROC: an open-source package for R and S+ to analyze and compare ROC curves. BMC Bioinform 2011;12:77.
[13] Pohlert T. PMCMRplus: Calc Pairwise Mult Comp Mean Rank Sums Ext 2023. R package version 1.9.10. https://CRAN.R-project.org/package=PMCMRplus.
[14] Jagust WJ, Mattay VS, Krainak DM, Wang S-J, Weidner LD, Hofling AA, et al. Quantitative brain amyloid PET. J Nucl Med 2024;65. jnumed.123.265766.
[15] Bucci M, Savitcheva I, Farrar G, Salvadó G, Collij L, Doré V, et al. A multisite analysis of the concordance between visual image interpretation and quantitative analysis of [18F]flutemetamol amyloid PET images. Eur J Nucl Med Mol I 2021;48:2183–99.
[16] Thurfjell L, Lilja J, Lundqvist R, Buckley C, Smith A, Vandenberghe R, et al. Automated quantification of 18F-flutemetamol PET activity for categorizing scans as negative or positive for brain amyloid: concordance with visual image reads. J Nucl Med 2014;55:1623–8.
[17] Matsuda H, Ito K, Ishii K, Shimosegawa E, Okazawa H, Mishina M, et al. Quantitative evaluation of 18F-flutemetamol PET in patients with cognitive impairment and suspected Alzheimer's disease: a multicenter study. Front Neurol 2021;11:578753.
[18] Mountz JM, Laymon CM, Cohen AD, Zhang Z, Price JC, Boudhar S, et al. Comparison of qualitative and quantitative imaging characteristics of [11C]PiB and [18F]flutemetamol in normal control and Alzheimer's subjects. NeuroImage 2F: Clin 2015;9:592–8.
[19] Fakhry-Darian D, Patel NH, Khan S, Barwick T, Svensson W, Khan S, et al. Optimisation and usefulness of quantitative analysis of 18F-florbetapir PET. Br J Radiol 2019;92:20181020.
[20] Nai Y-H, Tay Y-H, Tanaka T, Chen CP, Robins EG, Reilhac A, et al. Comparison of three automated approaches for classification of amyloid-PET images. Neuroinformatics 2022;20:1065–75.
[21] Rousset OG, Ma Y, Evans AC. Correction for partial volume effects in PET: principle and validation. J Nucl Med 2F: Publ Soc Nucl Med 1998;39:904–11.
[22] Klunk WE, Engler H, Nordberg A, Wang Y, Blomqvist G, Holt DP, et al. Imaging brain amyloid in Alzheimer's disease with Pittsburgh Compound-B. Ann Neurol 2004;55:306–19.
[23] Fodero-Tavoletti MT, Rowe CC, McLean CA, Leone L, Li Q-X, Masters CL, et al. Characterization of PiB binding to white matter in Alzheimer Disease and other dementias. J Nucl Med 2009;50:198–204.
[24] Lowe VJ, Lundt ES, Senjem ML, Schwarz CG, Min H-K, Przybelski SA, et al. White matter reference region in PET studies of 11 C-Pittsburgh compound B uptake: effects of age and amyloid-β deposition. J Nucl Med 2018;59:1583–9.
[25] Tanaka T, Stephenson MC, Nai Y-H, Khor D, Saridin FN, Hilal S, et al. Improved quantification of amyloid burden and associated biomarker cut-off points: results from the first amyloid Singaporean cohort with overlapping cerebrovascular disease. Eur J Nucl Med Mol Imaging 2020;47:319–31.
[26] Glodzik L, Rusinek H, Li J, Zhou C, Tsui W, Mosconi L, et al. Reduced retention of Pittsburgh compound B in white matter lesions. Eur J Nucl Med Mol Imaging 2015;42:97–102.
[27] Goodheart AE, Tamburo E, Minhas D, Aizenstein HJ, McDade E, Snitz BE, et al. Reduced binding of Pittsburgh compound-B in areas of white matter hyperintensities. NeuroImage: Clin 2015;9:479–83.
[28] Hashimoto T, Yokota C, Koshino K, Temma T, Yamazaki M, Iguchi S, et al. Binding of 11C-Pittsburgh compound-B correlated with white matter injury in hypertensive small vessel disease. Ann Nucl Med 2017;31:227–34.
[29] Collij LE, Bollack A, Joie RL, Shekari M, Bullich S, Roé-Vellvé N, et al. Centiloid recommendations for clinical context-of-use from the AMYPAD consortium. Alzheimer 19s Dement 2024.
[30] Iaccarino L, Burnham SC, Tunali I, Wang J, Navitsky M, Arora AK, Pontecorvo MJ. A practical overview of the use of amyloid-PET centiloid values in clinical trials and research. Neuroimage Clin 2025;46:103765.
[31] La Joie R, Ayakta N, Seeley WW, Borys E, Boxer AL, DeCarli C, et al. Multisite study of the relationships between antemortem [11C]PIB-PET centiloid values and postmortem measures of Alzheimer's disease neuropathology. Alzheimers Dement 2019;15(2):205–16. Feb.